Crystal structure of hexagonal SrAl$_2$O$_4$ at 1073 K

Koichiro Fukuda*, Kentaro Fukushima

Department of Environmental and Materials Engineering, Nagoya Institute of Technology, Nagoya 466-8555, Japan

Abstract

The crystal structure of SrAl$_2$O$_4$ at 1073 K was determined from conventional X-ray powder diffraction data using direct methods, and it was further refined by the Rietveld method. The structure was hexagonal (space group $P6_3$, $Z = 6$) with $a = 0.89260(3)$ nm, $c = 0.84985(2)$ nm and $V = 0.58639(3)$ nm^3. Final reliability indices were $R_{wp} = 7.87\%$, $R_p = 5.87\%$ and $R_B = 4.19\%$. The [AlO$_4$] tetrahedra are linked to form trigonally distorted rings and they are joined in layers. These layers are stacked with a two-layer repeat and connected by the tetrahedral apices. All of the Sr atoms occupy the centers of the rings when viewed along the c-axis. The structure is described as a stuffed derivative of tridymite.
© 2005 Elsevier Inc. All rights reserved.

Keywords: Strontium aluminate; High-temperature XRD; Rietveld method; Superstructure; Stuffed tridymite derivative

1. Introduction

Strontium aluminate (SrAl$_2$O$_4$) is one of the most promising host materials for long afterglow luminescence [1]. During heating this compound undergoes a phase transformation from monoclinic (space group $P2_1$) to hexagonal at 950 K [2]. The monoclinic structure [3] is well known to be stuffed tridymite derivative. The hexagonal structure at high temperatures has long been suggested to be isomorphous with that of BaAl$_2$O$_4$ [4].

At ambient temperature, BaAl$_2$O$_4$ is hexagonal (space group $P6_3$) having a superstructure with unit-cell parameters 2A and C [5,6], where A and C correspond to the lattice parameters of hexagonal tridymite. Upon heating, a phase transformation occurred over a wide temperature range of 400–670 K. The space group of the high-temperature phase has been determined by high-resolution transmission electron microscopy (TEM) to be $P6_322$ with the unit-cell parameters A and C [7].

A series of powder specimens in the BaAl$_2$O$_4$–SrAl$_2$O$_4$ system has been examined at ambient temperature by TEM to reveal another superstructure of $\sqrt{3}A$ and C

(probable space group $P6_3$) [8]. This superstructure, being recognized for the crystals with Ba/(Ba + Sr) = 0.9, 0.8 and 0.6, has not been elucidated so far.

Recently, Yamada et al. have investigated the crystal structure of Eu-doped SrAl$_2$O$_4$ (space group $P6_322$) at ambient temperature [9]. They refined the structure with X-ray powder diffraction data by the combined use of Rietveld method and maximum-entropy method (MEM) [10,11]. The electron density distribution (EDD) was expressed by the split-atom model, in which the oxygen atoms in the 2d and 6g sites were split over the lower symmetry sites 6h and 12i, respectively.

In the present study, we have determined the crystal structure of hexagonal SrAl$_2$O$_4$ at 1073 K from high-temperature powder XRD data. All of the reflection lines, including very weak superstructure reflections, were successfully indexed with the unit cell of $\sqrt{3}A$ and C.

2. Experimental

The present specimen of strontium aluminate SrAl$_2$O$_4$ was prepared from stoichiometric amounts of reagent-grade chemicals SrCO$_3$ and Al$_2$O$_3$. The mixture was

---

*Corresponding author. Fax: +81 52 735 5289.

E-mail address: fukuda.koichiro@nitech.ac.jp (K. Fukuda).

pressed into pellets (12 mm diameter and 3 mm thick), heated at 1773 K for 1 h, followed by quenching in air.

X-ray powder diffraction intensities were collected at 1073 K, the stable temperature region of the high-temperature phase, on a Rigaku RINT2000 diffractometer in the Bragg–Brentano geometry using monochromatized $CuK\alpha$ radiation (50 kV, 300 mA) and a step-scan technique with a 2θ range of 19–120° and a fixed counting time of 2 s/step and a step interval of 0.02°. The divergence slit of 0.5° was employed, which enabled us to collect the quantitative profile intensities in the 2θ range.

3. Results and discussion

3.1. Structure determination and refinement

Peak positions were determined after $K\alpha_2$ stripping on a computer program POWDERX [12], followed by the indexing procedure on a computer program TREOR90 [13]. In the latter procedure, 2θ values of 36 peak positions were used as input data. Only one hexagonal cell was found with satisfactory figures of merit $M_{20}/F_{20} = 70/68(0.01295, 23)$, $M_{30}/F_{30} = 50/49(0.01392, 0)$ and $M_{36}/F_{36} = 45/37(0.01393, 70)$ [14,15]. However, the derived unit cell ($a = 0.51555(2)$ nm and $c = 0.85054(7)$ nm) could index only the main reflections. All of the reflection lines, including very weak ones, were successfully indexed with a hexagonal superstructure of $\sqrt{3}A$ and C ($a = 0.8930$ nm and $c = 0.8505$ nm) as shown in Fig. 1.

The reflection intensities were examined to confirm the presence and absence of reflections. There were systematic absences $l \neq 2n$ for $000l$ reflections, implying that the possible space groups are $P6_3$, $P6_3/m$ and $P6_322$. All of the possible space groups were tested using the EXPO package [16] for crystal structure determination. A minimum reliability index R_F [17] of 13.9% was obtained with the space group $P6_3$ in a default run of the program. Structural parameters of all atoms were refined by the Rietveld method using the computer program RIETAN-2000 [18] (Fig. 2). The background intensities were fitted to a polynomial function with ten adjustable parameters. The split pseudo-Voigt function [19] was used to fit the peak profile. Isotropic atomic displacement parameters, B, were assigned to all atoms. Reliability indices [17] were $R_{wp} = 7.87\%$, $R_p = 5.87\%$ and $R_B = 4.19\%$. Crystal data are given in Table 1, and final positional and displacement parameters of atoms are given in Table 2.

3.2. Structure description

Fig. 3 shows a crystal structure of $SrAl_2O_4$ at 1073 K. The $[Al1O_4]$ and $[Al2O_4]$ tetrahedra are alternatively linked in trigonally distorted rings, with tetrahedra pointing up and down, to form layers perpendicular to the c-axis (Fig. 3(a)). These layers are stacked as in tridymite with a two layer repeat and joined by the
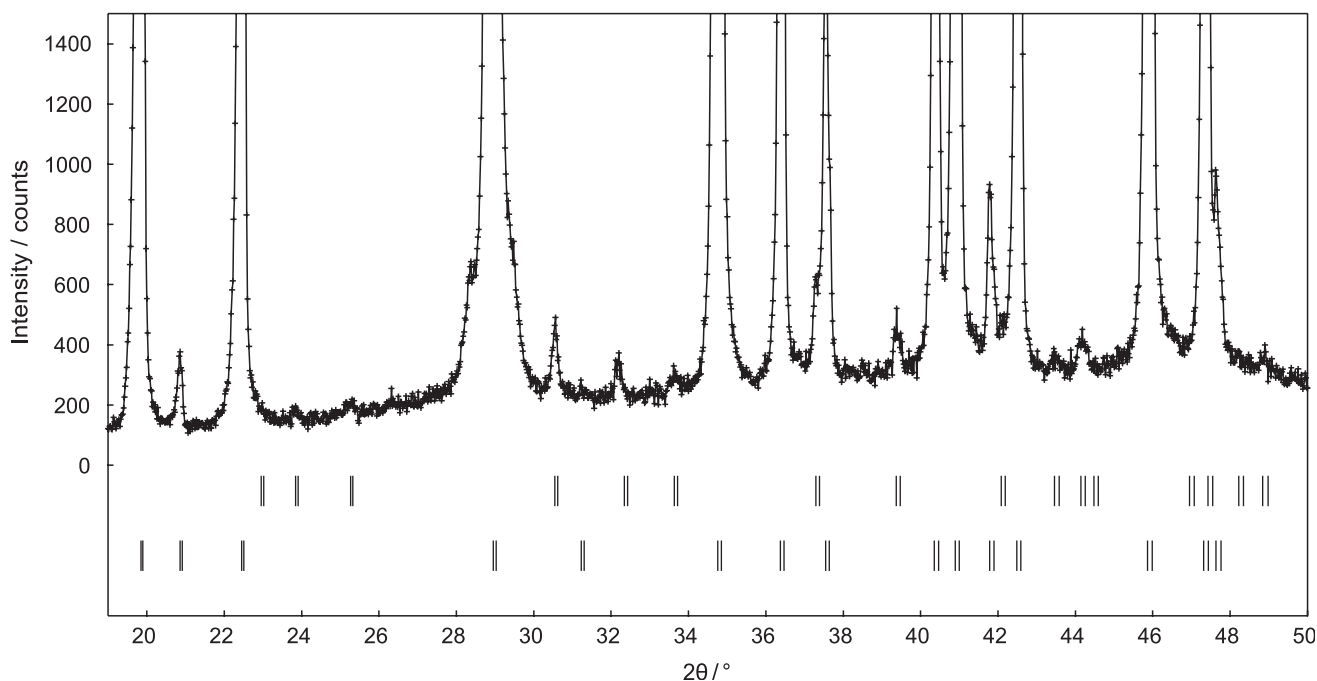

Fig. 1. Part of the observed (+ marks) pattern of $SrAl_2O_4$ at 1073 K. The upper and lower vertical marks indicate the positions of possible superstructure and substructure reflections, respectively.
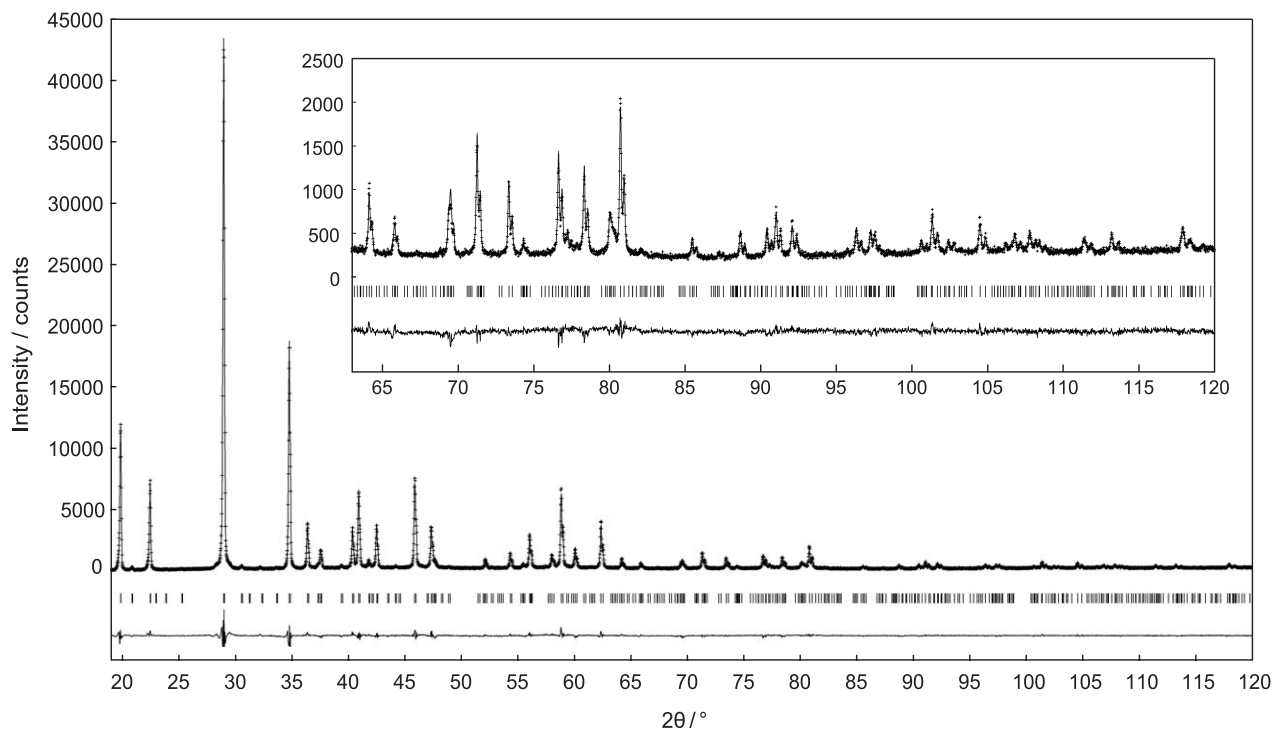
Fig. 2. Comparison between observed (+ marks) and calculated (upper solid line) patterns of $SrAl_2O_4$ at 1073 K. The difference curve is shown in the lower part of the figure. Vertical marks indicate the positions of possible Bragg reflections.

Table 1
Crystal data of strontium aluminate at 1073 K

Chemical composition	$SrAl_2O_4$
Space group	$P6_3$
a/nm	0.89260(3)
c/nm	0.84985(2)
V/nm^3	0.58639(3)
Z	6
D_X/Mgm^{-3}	3.49

Table 2
Structural parameters of $SrAl_2O_4$ at 1073 K

Atom	Site	x	y	z	B/nm^2
Sr1	2a	0	0	0	0.031(2)
Sr2	2b	1/3	2/3	−0.010(1)	0.032(1)
Sr3	2b	1/3	2/3	0.492(1)	0.032(1)
Al1	6c	0.332(2)	0.337(3)	0.685(3)	0.018(2)
Al2	6c	0.328(2)	0.335(3)	0.293(2)	0.026(3)
O1	6c	0.289(2)	0.356(3)	0.510(4)	0.063(5)
O2	6c	0.248(2)	0.126(2)	0.298(1)	0.013(5)
O3	6c	0.215(4)	0.790(5)	0.239(2)	0.042(10)
O4	6c	0.549(3)	0.093(4)	0.263(1)	0.027(9)

(a)

(b)

Fig. 3. Crystal structure of $SrAl_2O_4$ at 1073 K. Viewed along [0001] in (a) and [10$\bar{1}$0] in (b).

tetrahedral apices (Fig. 3(b)). The Sr atoms occupy, when viewed along [0001], the centers of the rings, where the triad axes exist parallel to the c-axis. Accordingly, the structure can be described as a stuffed derivative of
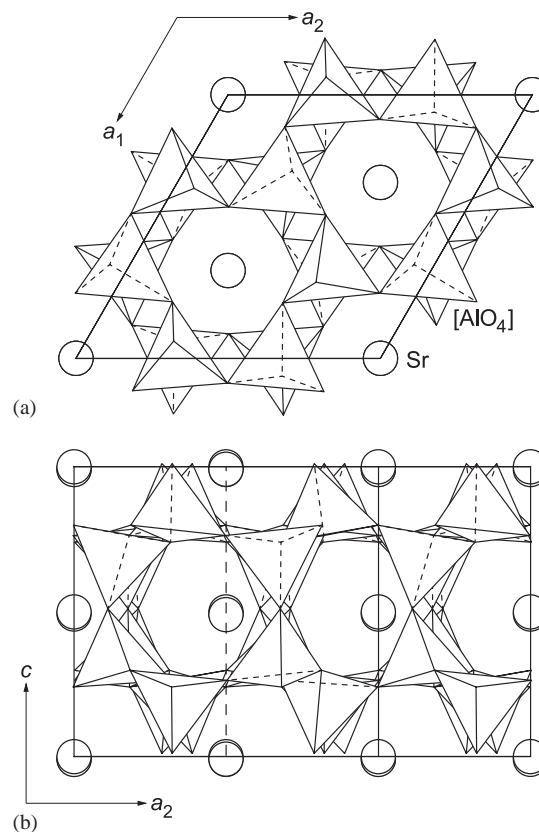
Table 3
Coordinates of Sr and Al

	O1[a]	O1[b]	O1[c]	O2	O2[d]	O2[e]	O2[a]	O2[b]	O2[c]
*Sr*1									
O1	2.92(2)	120(1)	120(1)	116.2(7)	94.4(7)	53.9(7)	56.5(7)	84.0(7)	135.8(7)
O1	5.06(2)	2.92(2)	120(1)	53.9(7)	116.2(7)	94.4(7)	135.8(7)	56.5(7)	84.0(7)
O1	5.06(4)	5.06(4)	2.92(3)	94.4(7)	53.9(7)	116.2(7)	84.0(7)	135.8(7)	56.5(7)
O2	5.18(2)	2.77(4)	4.48(4)	3.17(1)	63.0(7)	63.0(7)	169.1(9)	108.0(9)	108.0(9)
O2	4.48(3)	5.18(3)	2.77(3)	3.31(3)	3.17(2)	63.0(7)	108.0(9)	169.1(9)	108.0(9)
O2	2.77(3)	4.48(3)	5.18(3)	3.31(2)	3.31(3)	3.17(1)	108.0(9)	108.0(9)	169.1(9)
O2	2.62(3)	5.09(3)	3.69(3)	5.72(2)	4.66(2)	4.66(2)	2.57(1)	80.2(9)	80.2(9)
O2	3.69(3)	2.62(3)	5.09(4)	4.66(2)	5.72(3)	4.66(2)	3.31(3)	2.57(2)	80.2(9)
O2	5.09(2)	3.69(4)	2.62(3)	4.66(2)	4.66(2)	5.72(2)	3.31(2)	3.31(3)	2.57(1)

	O1[f]	O1[g]	O1[c]	O3	O3[h]	O3[i]	O4[f]	O4[g]	O4[c]
*Sr*2									
O1	3.48(2)	120(1)	120(1)	123.2(9)	86.5(9)	53.5(9)	94.4(8)	127.7(9)	54.3(8)
O1	6.02(4)	3.48(3)	120(1)	53.5(9)	123.2(9)	86.5(9)	54.3(8)	94.4(8)	127.7(9)
O1	6.02(2)	6.02(3)	3.48(1)	86.5(9)	53.5(9)	123.2(9)	127.7(9)	54.3(8)	94.4(8)
O3	5.55(5)	2.89(4)	4.34(4)	2.82(3)	70(1)	70(1)	108(1)	109(1)	177(1)
O3	4.34(3)	5.55(5)	2.89(3)	3.23(7)	2.82(3)	70(1)	177(1)	108(1)	109(1)
O3	2.89(5)	4.34(5)	5.55(3)	3.23(6)	3.23(4)	2.82(2)	109(1)	177(1)	108(1)
O4	4.55(5)	2.90(4)	5.54(4)	4.44(2)	5.50(4)	4.47(3)	2.68(2)	74(1)	74(1)
O4	5.54(4)	4.55(4)	2.90(4)	4.47(3)	4.44(3)	5.50(3)	3.21(3)	2.68(2)	74(1)
O4	2.90(3)	5.54(5)	4.55(3)	5.50(5)	4.47(2)	4.44(3)	3.21(6)	3.21(5)	2.68(3)

	O1	O1[h]	O1[i]	O3	O3[h]	O3[i]	O4[j]	O4[k]	O4[l]
*Sr*3									
O1	2.61(3)	120(1)	120(1)	125(1)	56(1)	97(1)	122.4(9)	82.2(9)	57.4(9)
O1	4.51(3)	2.61(1)	120(1)	97(1)	125(1)	56(1)	57.4(9)	122.4(9)	82.2(9)
O1	4.51(4)	4.51(2)	2.61(2)	56(1)	97(1)	125(1)	82.2(9)	57.4(9)	122.4(9)
O3	4.83(5)	4.09(4)	2.57(4)	2.84(3)	69(1)	69(1)	112(1)	113(1)	178(1)
O3	2.57(4)	4.83(3)	4.09(5)	3.23(7)	2.84(3)	69(1)	178(1)	112(1)	113(1)
O3	4.09(4)	2.57(4)	4.83(4)	3.23(6)	3.23(4)	2.84(2)	113(1)	178(1)	112(1)
O4	4.88(4)	2.69(4)	3.67(3)	4.81(2)	5.80(3)	4.83(3)	2.95(2)	66(1)	66(1)
O4	3.67(5)	4.88(3)	2.69(4)	4.83(3)	4.81(3)	5.80(3)	3.21(3)	2.95(2)	66(1)
O4	2.69(3)	3.67(4)	4.88(5)	5.80(4)	4.83(2)	4.81(3)	3.21(6)	3.21(5)	2.96(3)

	O1		O2[l]		O3[m]		O4[l]
*Al*1							
O1		1.56(4)		107(1)		123(2)	107(1)
O2		2.77(3)		1.89(2)		107(1)	103(1)
O3		2.89(5)		2.91(5)		1.73(5)	109(2)
O4		2.69(3)		2.86(3)		2.86(6)	1.78(3)

	O1		O2		O3[h]		O4[n]
*Al*2							
O1		1.56(4)		107(1)		123(2)	107(1)
O2		2.77(3)		1.89(2)		107(1)	103(1)
O3		2.89(5)		2.91(5)		1.73(5)	109(2)
O4		2.69(3)		2.86(3)		2.86(6)	1.78(3)

The values in diagonals are the central atom–ligand distances (Å), in the upper-right triangle the bond angles (deg) and in the lower left the ligand–ligand distances (Å) are given.
Symmetry transformations used to generate equivalent atoms: (a) $-x$, $-y$, $-1/2+z$; (b) y, $-x+y$, $-1/2+z$; (c) $x-y$, x, $-1/2+z$; (d) $-y$, $x-y$, z; (e) $-x+y$, $-x$, z; (f) $1-x$, $1-y$, $-1/2+z$; (g) y, $1-x+y$, $-1/2+z$; (h) $1-y$, $1+x-y$, z; (i) $-x+y$, $1-x$, z; (j) $1-x$, $1-y$, $1/2+z$; (k) y, $1-x+y$, $1/2+z$; (l) $x-y$, x, $1/2+z$; (m) $1+x-y$, x, $1/2+z$; (n) $1-x+y,1-x,z$.

tridymite, in which all of the Si^{4+} is replaced by Al^{3+} and the charge compensating cation Sr^{2+} occupy the channels between the rings of tetrahedra.

Selected interatomic distances and bond angles, together with their standard uncertainties, are listed in Table 3. Ionic radii of Al^{3+} in the fourfold coordination

$[r(Al^{3+}) = 0.039$ nm and $r(O^{2-}) = 0.138$ nm] predict the interatomic distance of 0.177 nm for Al–O [20]. With monoclinic $SrAl_2O_4$, the mean Al–O bond length is 0.175 nm [3]. These values are in good agreement with the mean interatomic distances of 0.174 nm for Al1–O and 0.173 nm for Al2–O. The Sr atom is ninefold coordinated, as in the monoclinic $SrAl_2O_4$ [3], with the mean Sr–O distance of 0.289 nm. This is in fair agreement with the mean Sr–O distance in monoclinic $SrAl_2O_4$ (0.286 nm).

3.3. Comparison in crystal structure with stuffed tridymite derivatives

The monoclinic $SrAl_2O_4$, being stable at temperatures below about 950 K, is a distorted form of the hexagonal $SrAl_2O_4$ (Fig. 4(a) and (b)). The space group change from $P6_3$ to its subgroup $P2_1$ eliminates the triad axis of the former phase. Thus, the distortion involves a reduction in the symmetry of the trigonally distorted rings. The disappearance of the triad axis would also result in the formation of three twin domains, which is related to the other by the lost symmetry axis. The presence of such a twin microtexture was actually confirmed by TEM in the crystals quenched from 1873 K [21].

The crystal structures of hexagonal $SrAl_2O_4$ and $BaAl_2O_4$ differ distinctly in the linkage pattern of the $[AlO_4]$ tetrahedra. In the former structure, all of the tetrahedral rings are equivalent and trigonally distorted. In the latter, there are two types of tetrahedral rings; trigonal rings and asymmetrical rings (Fig. 4(c)). The trigonal rings, comprising 25% of the total number of rings, contain in their centers the Ba atoms with the special position (2a). This implies that the triad axes exist in the centers of the rings, and hence they are distorted trigonally as in the hexagonal $SrAl_2O_4$. On the other hand, the Ba atoms in the asymmetrical rings are located at the general position (6c) site. The alternating arrangement of these two types of rings within the layers leads to a doubling of the a-axis with respect to the tridymite unit cell.

In our preliminary analysis of the present powder XRD data, we have tried a structural refinement using the split-atom model (space group $P6_322$) with the unit-cell parameters A and C [9]. In spite of the wrong choice of the space group as well as the unit-cell dimensions, the reliability indices considerably decreased after the Rietveld refinement; the final indices without excluding any regions in the diffraction data were $R_{wp} = 8.61\%$, $R_p = 6.27\%$ and $R_B = 4.19\%$. In order to visualize the EDD, MEM was subsequently applied on a computer program PRIMA [18]. The EDD of oxygen ions at $6h$ site demonstrated the three sharp maximum around the threefold axis, and the $12i$ site showed elongated EDD nearly along the c-axis. The positional disorder of these
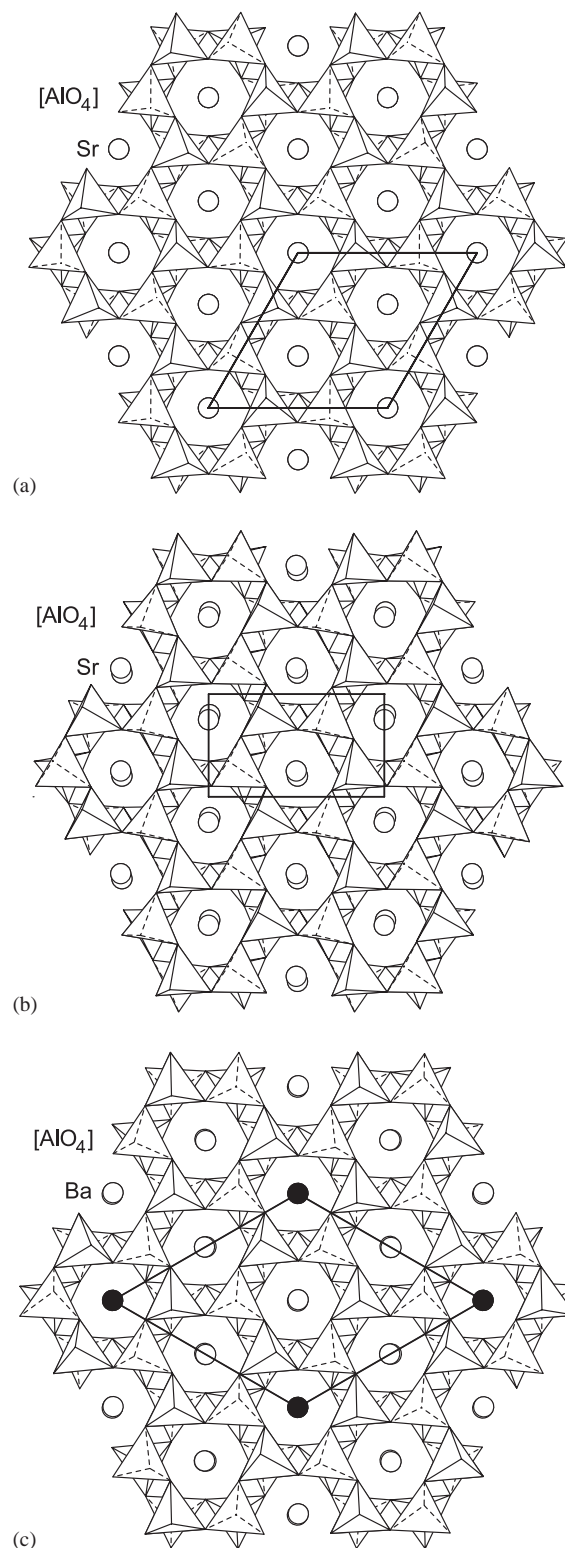

Fig. 4. Comparison of linkage patterns of the $[AlO_4]$ tetrahedra. (a) Hexagonal $SrAl_2O_4$ (space group $P6_3$) viewed along [0001], (b) monoclinic $SrAl_2O_4$ ($P2_1$) projected onto (100) and (c) $BaAl_2O_4$ ($P6_3$) viewed along [0001]. The solid lines depict the unit cells. The closed circles in (c) indicate Ba atoms at the special position (2a) site.

oxygen ions is consistent with that as determined in Eu-doped $SrAl_2O_4$ [9]. The oxygen ions at $6h$ site correspond to O1 (Table 2) in the present superstructure ($\sqrt{3}A$, C), and those at $12i$ site correspond to O2, O3 and O4.

4. Conclusion

We determined the crystal structure of $SrAl_2O_4$ at 1073 K, being hexagonal with space group $P6_3$. The Al atoms are coordinated to four oxygen atoms at a mean distance of 0.173 nm. The Sr atom is 9-fold coordinated with a mean Sr–O distance of 0.289 nm. The crystal structure can be described in terms of layers formed from [AlO$_4$] tetrahedra linked to form trigonally distorted rings. These layers are stacked and connected by the tetrahedral apices to give a three-dimensional structure. The Sr atoms all occupy the centers of the rings when viewed along the c-axis. The linkage pattern of the [AlO$_4$] tetrahedra was compared to those of the monoclinic $SrAl_2O_4$ and $BaAl_2O_4$ in order to characterize the crystal structure of the hexagonal $SrAl_2O_4$.

Acknowledgment

References

[1] H. Takasaki, S. Tanabe, T. Hanada, J. Ceram. Soc. Jpn. 104 (1996) 322–326.
[2] C.M.B. Henderson, D. Taylor, Mineral. Mag. 45 (1982) 111–127.
[3] A.R. Schulze, H. Mueller-Buschbaum, Z. Anorg. Allg. Chem. 475 (1981) 205–210.
[4] S. Ito, S. Banno, K. Suzuki, M. Inagaki, Z. Phys. Chem. Neue Folge 105 (1977) 173–178.
[5] W. Hoerkner, H. Mueller-Buschbaum, Z. Allg. Chem. 451 (1979) 40–44.
[6] S.-Y. Huang, R. vonder Muehll, R. Ravez, M. Couzi, J. Solid State Chem. 109 (1994) 97–105.
[7] A.M. Abakumov, O.I. Lebedev, L. Nistor, G. Van Tendeloo, S. Amelinckx, Phase Transitions 71 (2000) 143–160.
[8] U. Rodehorst, M.A. Carpenter, S. Marion, C.M.B. Henderson, Mineral. Mag. 67 (2003) 989–1013.
[9] H. Yamada, W.S. Shi, C.N. Xu, J. Appl. Crystallogr. 37 (2004) 698–702.
[10] M. Takata, E. Nishibori, M. Sakata, Z. Kristallogr. 216 (2001) 71–86.
[11] F. Izumi, S. Kumazawa, T. Ikeda, W.-Z. Hu, A. Yamamoto, K. Oikawa, Mater. Sci. Forum 378–381 (2001) 59–64.
[12] C. Dong, J. Appl. Crystallogr. 32 (1999) 838.
[13] P.E. Werner, L. Eriksson, M. Westdahl, J. Appl. Crystallogr. 18 (1985) 367–370.
[14] P.M. de Wolff, J. Appl. Crystallogr. 1 (1968) 108–113.
[15] G.S. Smith, R.L. Snyder, J. Appl. Crystallogr. 12 (1979) 60–65.
[16] A. Altomare, M.C. Burla, M. Camalli, B. Carrozzini, G.L. Cascarano, C. Giacovazzo, A. Guagliardi, A.G.G. Moliterni, G. Polidori, R. Rizzi, J. Appl. Crystallogr. 32 (1999) 339–340.
[17] R.A. Young, in: R.A. Young (Ed.), The Rietveld Method, Oxford University Press, Oxford UK, 1993, pp. 1–38.
[18] F. Izumi, T. Ikeda, Mater. Sci. Forum 198 (2000) 321–324.
[19] H. Toraya, J. Appl. Crystallogr. 23 (1990) 485–491.
[20] R.D. Shannon, Acta Crystallogr. A 32 (1976) 751–767.
[21] J. Barbier, J. Neuhausen, Eur. J. Mineral 2 (1990) 273–282.